Heterogenization of a Molecular Ni Catalyst within a Porous Macroligand for the Direct C-H Arylation of Heteroarenes

Yorck Mohr, Marcelo Alves-Favaro, Rémy Rajapaksha, Gaëlle Hisler, Alisa Ranscht, Partha Samanta, C. Lorentz, Mathis Duguet, Caroline Mellot-Draznieks, Elsje Quadrelli, et al.

Heterogenization of a molecular Ni catalyst within a porous macroligand for the direct C-H arylation of heteroarenes

Yorck Mohr,[†] Marcelo Alves-Favaro,[†] Rémy Rajapaksha,[†] Gaëlle Hisler,[†] Alisa Ranscht,[†] Partha Samanta,[†] Chantal Lorentz,[†] Mathis Duguet,[‡] Caroline Mellot-Draznieks,[‡] Elsje Alessandra Quadrelli,[†] Florian M. Wisser*[,†,§] and Jérôme Canivet*[,†]

[†]Univ. Lyon, Université Claude Bernard Lyon 1, CNRS, IRCELYON - UMR 5256, 2 Av. Albert Einstein, 69626 Villeurbanne, France.

[‡]Laboratoire de Chimie des Processus Biologiques (LCPB) Collège de France, PSL Research University, CNRS Sorbonne Université, 11 Place Marcelin Berthelot, 75231 Paris Cedex 05, France

[§]Institute of Inorganic Chemistry, University of Regensburg, 93040 Regensburg, Germany.

ABSTRACT: Direct C-H functionalization catalyzed by a robust and recyclable heterogeneous catalyst is highly desirable for sustainable fine chemical synthesis. Bipyridine units covalently incorporated into the backbone of a porous organic polymer were used as a porous macroligand for the heterogenization of a molecular nickel catalyst. A controlled nickel loading within the porous macroligand is achieved and the nickel coordination to the bpy sites is assessed at the molecular level using IR and solid-state NMR spectroscopy. The heterogenized Ni-bpy catalyst was successfully applied to the direct and fully selective C2 arylation of benzothiophenes, thiophene and selenophene, as well as for the arylation of free NH-indole. Recyclability of the catalyst was achieved by employing hydride activators to reach a cumulative turnover number of more than 300 after seven cycles of catalysis, which corresponds to a total productivity of 12 grams of 2-phenylbenzothiophene, chosen as model target biaryl, per gram of catalyst.

1. INTRODUCTION

The use of earth-abundant metals (EAM) for the direct C-H activation through a heterogeneous protocol would allow reaching appealing sustainability for the synthesis and derivatization of fine chemicals[1,2] since this approach would enable at the same time (i) the use of accessible resources, (ii) a beneficial atom- and step-economy of non-activated substrates, and (iii) the ability to reuse the catalyst and to easily separate it from products.[3–8]

The direct C-H arylation of heteroarenes is a key reaction for the synthesis of advanced heterobiaryls compounds.[9–11] In particular, the arylation of benzothiophene[12] is highly desirable because the (aryl)benzothiophene motif is widely present in active pharmaceutical ingredients (API) of marketed drugs[13–15] and in optoelectronic performance materials found in organic light-emitting diodes, organic field effect transistors and organic photovoltaic solar cells.[16–19] Moreover, the regioselective derivatization is of a paramount importance for structure-related activity.[20] In the case of (benzo)thiophene C2-H selective arylation, reported protocols were mostly restricted to homogeneous platinum group metal (PGM) catalysts,[21–24] with far less examples using EAM catalysts.[25,26] Aiming at developing EAM catalysts for C–H arylation reactions, we recently reported a novel homogeneous Ni-based catalytic system for the regioselective direct C2-H arylation of heteroarenes.[27]

To change the paradigm of molecular catalytic processes for fine chemical synthesis, we introduced recently the concept of solid porous macroligand for heterogenized molecular catalysis.[28] Having molecularly-defined active sites, porous macroligands have been found to drive the activity and the selectivity of heterogenized catalytic processes on a similar way as molecular ligands[29] but with the advantage of the structuration in a three-dimensional framework[30,31] and the confinement within a porous nanospace.[32,33]

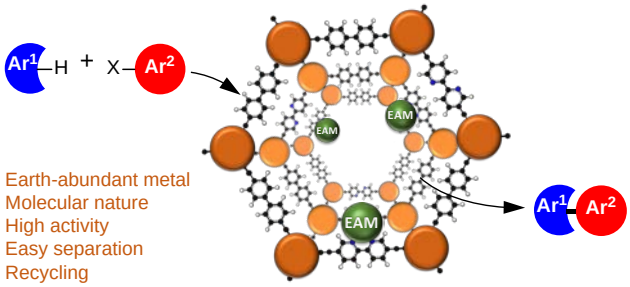

Scheme 1. Porous macroligands for heterogenized earth-abundant metal (EAM) molecular C-H arylation catalyst.

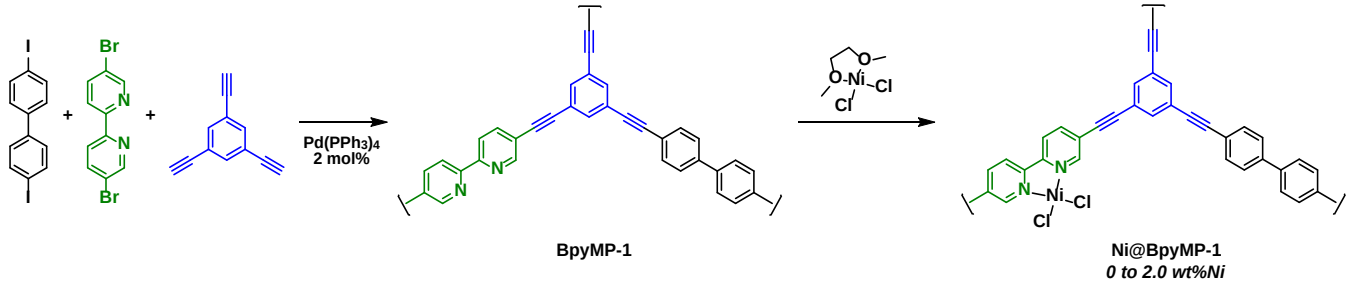

Scheme 2. Synthesis of the Ni@BpyMP-1 catalysts series.

Among organo-based porous materials offering functional derivatizable building blocks, porous organic polymers (POPs) are appealing platforms for the design of porous macroligands due to their chemical robustness arising from their covalent C-C bonds network. Such stable network appear to be well suited to the strong basic conditions used in the homogeneous Ni-catalyzed benzothiophene C-H arylation reaction.[27] Furthermore, POP-type materials were already reported for the immobilization of nickel catalyst for the ethylene oligomerization,[34] or for Suzuki-Miyaura coupling.[35]

While proof-of-concept heterogeneous C-H activation catalysts were recently published by the group of Yamada for palladium-catalyzed thiophene arylation[36] and by the group of Sawamura for nickel-catalyzed benzoxazole arylation,[37] a general protocol is still missing.

Here we report the heterogenization of an earth-abundant molecular nickel complex within the structure of a bipyridine (bpy)-based POP, namely BpyMP-1, used as a porous macroligand.[29,38] The molecularly-defined Ni@BpyMP-1 heterogeneous catalyst allows the C2-selective arylation of benzothiophene and thiophene and, to the best of our knowledge, the first heterogeneous C2-selective arylation of selenophene. Furthermore its efficient reuse is highlighted.

2. RESULTS AND DISCUSSION

2.1 Catalysts synthesis and characterizations.

The BpyMP-1 is a bpy-containing porous polymer synthesized from a protocol first developed by the group of Thomas for non-functionalized POPs[39] and adapted by our group for a mixed monomers approach (Scheme 2).[29,38] The nickel infiltration was carried out in anhydrous methanol using a Ni(II) salt bearing a labile ethereal ligand (glyme).[40] Six different infiltrations were conducted with varying amounts of nickel in order to reach different bpy binding site occupancies.

The resulting Ni@BpyMP-1 solids and the pristine BpyMP-1 were fully characterized by ^{1}H and ^{13}C solid-state NMR spectroscopy, IR spectroscopy, nitrogen physisorption experiments as well as by ICP-OES analysis.

ICP-OES analysis revealed the following metalation ratios: 0.43, 0.64, 1.10, 1.29, 1.71 and 2.02 wt%; the catalysts are named accordingly (Table 1). While for low Ni loadings almost complete Ni incorporation is reached, for high Ni loadings a significantly lower loading than the theoretical one is achieved. The pristine polymer as well as the different Ni-loaded materials show a permanent porosity towards nitrogen in nitrogen physisorption experiments at 77 K (Table 1 and Figure S1). The isotherms of all materials show the characteristic swelling behavior of microporous polymers. With increasing nickel loading the apparent surface area (SA_{BET}) and pore volume (V_{tot}) decrease from approx. 760 m^2/g to 680 m^2/g for pristine BpyMP-1 and 2.02wt%Ni@BpyMP-1 respectively (Table 1).

Table 1. Summary of N_2 physisorption and ICP-OES data as well as the calculated binding site occupancy for the nickel infiltration into BpyMP-1.

catalyst	SA_{BET} (m^2/g)	V_{tot} (cm^3/g)	w_{Ni} (wt%)	w_{Pd} (wt%)[a]
BpyMP-1	762	0.49	0	0.59
0.43w%Ni@BpyMP-1	754	0.45	0.43	0.58
0.64w%Ni@BpyMP-1	749	0.45	0.64	0.56
1.10w%Ni@BpyMP-1	736	0.43	1.10	0.54
1.29w%Ni@BpyMP-1	728	0.42	1.29	0.52
1.71wt%Ni@BpyMP-1	700	0.41	1.71	0.49
2.02wt%Ni@BpyMP-1	684	0.39	2.02	0.42

[a] All polymers contain approx. 0.5 wt% palladium stemming from a mechanical or chemical trapping of the palladium catalyst used for polymer synthesis.[41]

IR spectroscopy indicates a very high yet not complete degree of polymerization : the diagnostic band of unreacted terminal ethynyl moieties, i.e. the asymmetric C≡C stretching vibration at 2100 cm^{-1}, is not observed, but the band corresponding to the more IR-sensitive alkynyl C-H stretching vibration at 3300 cm^{-1} has not completely disappeared (Figure S2).[39]

To shine light on the composition of the porous polymer, quantitative ^{13}C composite-pulse multiple cross polarization (ComPmultiCP) NMR spectra were recorded.[42,43] In the spectra of pristine BpyMP-1, the broad signal at approx. 90 ppm is attributed to medial triple bonds, while the weak signals at 82 and 78 ppm correspond to unreacted terminal ethynyl moieties (Figure 1).[39] Deconvolution of the signals reveals that less than 4 % of unreacted ethynyl groups remain in the polymer.

The NMR signals around 155 ppm are attributed to the carbon atoms in the 2/2' and 6/6' position in the bipyridine moiety,[29] indicating that approx. 75 % of the bipyridine based monomer is incorporated into the final polymer with respect to the triethynylbenzene core.

Upon nickelation the signal intensities for those C-atoms decrease, most likely caused by the influence of paramagnetic Ni^{2+} atoms on the ^{13}C chemical shifts of carbon atoms close to it.[44–46]

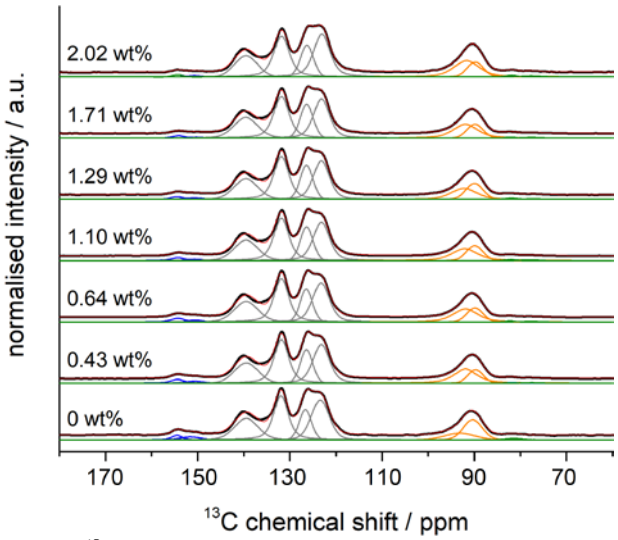

Figure 1. ^{13}C ComPmultiCP MAS NMR spectra of BpyMP-1 materials with varying amounts of nickel loading. Color code of deconvolution: blue: carbon atoms next to the bipyridine N atom; grey: other aromatic carbon atoms; orange: medial alkyne carbon atoms; green: terminal ethynyl groups. Deconvolution was done using DMFit software.[47] Complete spectra are shown in the Supporting Information, section S4.3.5.

2.2 Assessment of nickel coordination to bpy sites. The vanishing of the ^{13}C NMR signals at around 155 ppm indicates a close spatial proximity between bpy units and paramagnetic Ni^{2+} centers, pointing toward a Ni-bpy coordinative interaction. We used this decrease in signal intensity, due to the paramagnetic effect of Ni on neighboring carbon atoms, to quantify the amount of bipyridine sites of the porous macroligand coordinating to one Ni atom and compare it with the nickel loading measured through ICP-OES analysis. The bpy occupancy was calculated from the ratio of normalized NMR signal integrals at 155 ppm between the pristine BpyMP-1 and the corresponding Ni-loaded polymer (Figures S3 and S4).

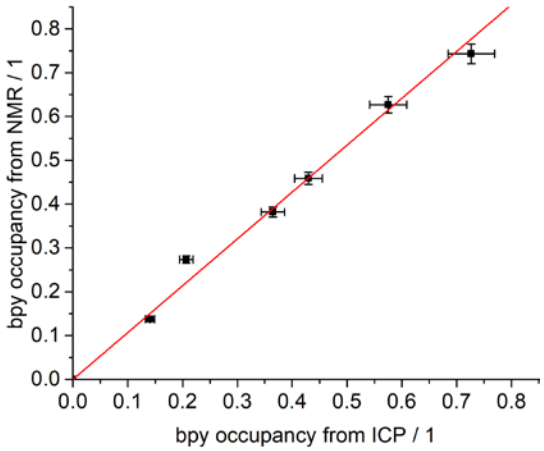

Figure 2. Correlation between bpy site occupancy as determined by ^{13}C ComPmultiCP MAS NMR and the Ni loading in wt% by ICP-OES analysis.

Thus the estimated bpy occupancy extracted from NMR data increases linearly with the Ni loading, reaching a maximum value of 74 ± 5% occupancy of bipyridine sites. The results are in agreement with the occupancy estimated by ICP-OES analysis and calculated from the ratio between bypiridine and nickel content within the polymer (Table S1, Figure S5 and Figure 2) To further corroborate the Ni interaction with the bpy-binding sites, IR spectra of the BpyMP-1 based catalysts, as well as molecular counter parts, were recorded. The band for the C-H deformation vibration of the bipyridine moiety at 1453 cm^{-1} decreased in intensity with increasing nickel loading (Figure 3a). DFT calculations on molecular cluster models of the binding site confirm the dependence of this band intensity to the bipyridine nickelation (Supporting Information, section S4.5 for further discussion). Similarly the C-H deformation vibration of molecular bipyridine at *ca.* 1440 cm^{-1} vanishes upon the formation of nickel(II) bipyridine complex (Supporting Information, section S4.3.4).[48,49] At the same time, the band at approx. 1465 cm^{-1}, attributed to the in-plane C-H vibration of the Ni(bpy) moiety,[50] increases in intensity.

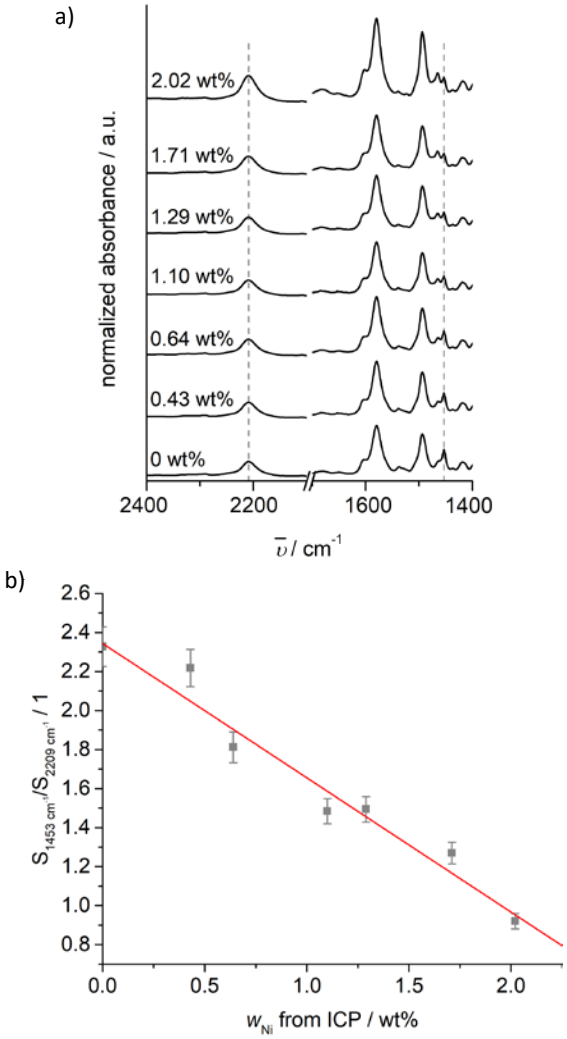

Figure 3. a) IR spectra of BpyMP-1 materials with varying amounts of Nickel loading between 2400 and 1400 cm^{-1}. The band at 1453 and 2209 cm^{-1} are highlighted. **b)** Linear correlation of normalized band intensity at 1453 cm^{-1} as a function of nickel loading.

As shown in Figure 3b, the ratio between the peak intensity of the band at 1453 cm^{-1} and that of the band at 2209 cm^{-1}, corresponding to internal C≡C bond used as unaffected reference vibration for all presented materials, displays a linear correlation with the Ni loading. Thus the decrease in band intensity at 1453

cm^{-1} is an additional descriptor of the Ni coordination to bpy sites. Overall, these descriptors demonstrate that each infiltrated nickel center is coordinated to a bpy unit and not physisorbed within the polymer and confirm the molecular nature of the Ni(bpy) sites.

2.3 Heterogeneous benzothiophene C-H arylation. We then explored the catalytic potential of Ni@BpyMP-1 for the direct C-H arylation of benzothiophene in the presence of lithium bis(trimethylsilyl)amide (LiHMDS)[27] in toluene (Scheme 3 and Table 2 entry 1).

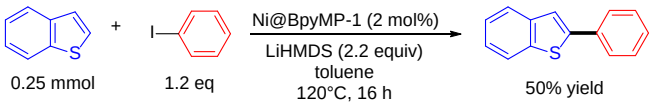

Scheme 3. Heterogeneous Ni-catalyzed direct and selective C2 arylation of benzothiophene.

The 2-phenylbenzothiophene was obtained with 50% yield and 100% regioselectivity for the arylation of benzothiophene at the C2 position using 2.02wt%Ni@BpyMP-1 catalyst (2 mol% of Ni with respect to benzothiophene). As compared to the homogeneous system (Table 2, entry 2),[27] the heterogeneous catalyst 2.02wt%Ni@BpyMP-1 retains the high regioselectivity of the reaction, albeit with a slightly lower yield. The heterogenization of the catalytic system within a porous polymer also allows a threefold decrease of the formation of the *N*-phenyl-*bis*(trimethylsilyl)amine (Ph-HMDS), side product from the reaction between iodobenzene and LiHMDS, compared to the homogeneous reaction (6% conversion of iodobenzene instead of 18%; see Supporting Information, Table S3 and section S5.3 for details). The pristine BpyMP-1, without any Ni, leads to no conversion and confirms that the catalytic activity arises from nickel-based catalyst within the porous matrix (Table 2 entry 3, 1% yield of 2-phenylbenzothiophene being observed most likely due to residual palladium from polymer synthesis). Hot filtration test also shows that no residual catalytic activity remains in the catalytic solution after removal of the solid catalyst (Figure S12).

Under homogeneous conditions, the reaction yield could be further enhanced by replacing toluene with ethereal solvents such as dioxane.[27] Unfortunately, almost no catalytic activity could be observed under heterogeneous conditions using ethereal solvents (Table 2, entries 4-7). The detrimental effect of dioxane as solvent is also evidenced in reaction performed in a mixture where the reaction yield drastically dropped from 50% in pure toluene to 25% and 5% when toluene contained 1 vol% and 10 vol% of dioxane, respectively (see Table S3).

Table 2. Summary of the nickel-catalyzed direct C2 arylation of benzothiophene under homogeneous and heterogeneous conditions.[a]

Entry	*Catalyst*	*Ni (mol%)* [b]	*solvent*	*2-Ph-BT yield (%)*
1	2.02wt%Ni@BpyMP-1 [c]	2	toluene	50
2	Ni(bpy)Cl_2	2	toluene	60
3	BpyMP-1 [c]	0	toluene	1
4	2.02wt%Ni@BpyMP-1 [c]	2	dioxane	1
5	2.02wt%Ni@BpyMP-1 [c]	2	THF	2
6	2.02wt%Ni@BpyMP-1 [c]	2	2-Me-THF	4
7	2.02wt%Ni@BpyMP-1 [c]	2	diglyme	1

[a] Reaction conditions: 0.25 mmol benzothiophene, 1.2 equiv iodobenzene, 2.2 equiv LiHMDS, θ = 120°C, t = 16 h; [b] relative to benzothiophene; [c] a constant mass of 13.5 mg of POP was used.

Using a constant mass of solid catalyst, the yield of the reaction increased first to reach a plateau for nickel loadings higher than 1 mol% of Ni with respect to benzothiophene (Figure 4), corresponding to loading of approx. 1 wt% Ni within the catalyst under the established conditions (see Table 2). Consequently, the turnover number (TON), calculated as the number of moles of 2-phenyl-benzothiophene formed per mole of Ni, decreased with increasing Ni loadings. A possible explanation might be a restricted access to active sites in the core of the polymer particle for higher Ni loadings. Even if the highest yields are obtained for 1.71wt% Ni@BpyMP-1 and 2.02wt%Ni@BpyMP-1, the best compromise between activity and yield is around 1 wt% Ni loading. Advantageously, the decrease in Ni loading suppressed the side product formation to less than 3% of the iodobenzene (into mainly Ph-HMDS, Table S3).

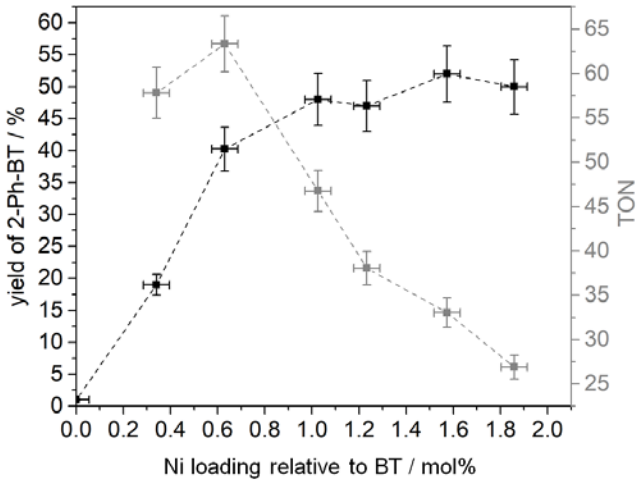

Figure 4. Yield in 2-Ph-BT for the heterogeneously catalyzed direct arylation of benzothiophene with varying amounts of Ni within a constant quantity of BpyMP-1 matrix (13.5 mg); reaction conditions: 0.25 mmol benzothiophene, 1.2 equiv iodobenzene, 2.2 equiv LiHMDS, T = 120°C, t = 16 h, 2 ml toluene.

In order to evaluate the stability and integrity of the aromatic polymer network under catalytic C-H arylation conditions, the reaction was performed using $^{13}C_6$-labelled iodobenzene over Ni@BpyMP-1. The ^{13}C NMR spectrum of the corresponding spent catalyst is dominated by three broad signals belonging to

the carbon atoms of iodobenzene-$^{13}C_6$, thus showing the integration of some phenyl groups into the backbone of the catalyst after the first catalytic run (Table S5). At the same time, the signature of terminal ethynyl groups is no longer detectable, the signals at 78 and 82 ppm in the ^{13}C ComPmultiCP MAS NMR spectra as well as the vibration at 3300 cm^{-1} in the IR spectra disappeared (Figures S9 and S10). Thus, it can be postulated that residual terminal ethynyl C-H bonds of the BpyMP-1 polymer are arylated due to their reaction with LiHMDS and iodobenzene, even in the absence of nickel (Figure S9), and no further arylation occurs at the C≡C bonds or at the aromatic building units.
In addition, the catalyst retains its porosity after catalysis (see Supporting Information, sections S5.4).

2.4 Catalyst reactivation. Then, we evaluated the ability of Ni@BpyMP-1 solids to be recycled in the C2 arylation of benzothiophene. A simple reuse of Ni@BpyMP-1 catalyst led only to traces of product (see Table S3).[51,52] The absence of significant decoordination of the nickel from the bpy site under standard reaction conditions was confirmed by solid-state NMR spectroscopy (see section S5.4.3, Figure S11). Nickel species could progressively become inaccessible by coordination of HMDS moieties, to form Ni(bpy)$(HMDS)_x$ species.[53] Since the molecular benzothiophene C-H arylation is proposed to occur through a redox pathway (believed to involve Ni(I)/Ni(III) species, even if a Ni(0)/Ni(II) redox catalysis cannot be ruled out),[27] we also postulate an irreversible nickel oxidation as deactivation pathway in the heterogeneous system. In order to reactivate the Ni species, we thus tested reducing agents including diisobutylaluminum hydride (DiBAlH) and sodium borohydride ($NaBH_4$),[54] since most of molecular Ni-based catalytic system for C-H arylation employ an additional reducing agent such as metallic zinc or a silver salt in stoichiometric amounts compared to the substrate.[55,56] Substantial catalytic activity is thus recovered (Figure 5). Interestingly, when reducing agents are used with the fresh catalyst, the activity for the first run drops to approx. 80% of the activity of the activator-free system, but remains stable for several consecutive cycles. Using 2wt%Ni@BpyMP-1 stable TONs of approx. 21 ± 2 were observed over seven cycles yielding total TONs of 160 and 148 in the presence of DiBAlH and $NaBH_4$ respectively (Figures S13 and S14). The TON could be further increased to approx. 44 per run using 1.10wt%Ni@BpyMP-1 in the presence of $NaBH_4$ (Figure 5). Thus after seven consecutive catalytic runs, a cumulative TON of 316 was reached. This corresponds to a total productivity of 12 grams of 2-phenylbenzothiophene per gram of catalyst.

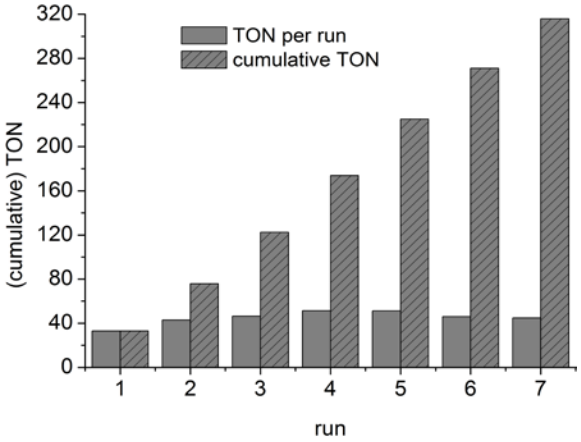

Figure 5. Graphical representation of TON value per run and the evolution of the cumulative TON. Reaction conditions: 0.25 mmol benzothiophene, 13.5 mg 1.10wt%Ni@BpyMP-1 (1 mol% Ni relative to benzothiophene), 2.2 equiv iodobenzene, 2.2 equiv LiHMDS, 2 ml of toluene, 16 h, 120°C. Before each run, the catalyst was treated with 0.25 mmol of $NaBH_4$ at 50°C for 20 min.

ICP-OES analysis of the reaction supernatant reveals a weak leaching of nickel from the catalyst to the catalytic solution of ca. 1.5 ppm for the first runs, which decreases rapidly to finally less than 0.5 ppm. After seven consecutive runs, 93% of the initial amount of nickel remain loaded within the catalyst (Figure S15, Tables S7 and S8).
Hot filtration test was carried out to demonstrate that the catalytic activity does not arise from leached Ni species (Figure S16). Also neither DiBAlH nor $NaBH_4$ itself catalyze the reaction in the absence of nickel (Table S3).

2.5 Scope of applicable substrates. Once the molecular nature of the nickel site and its ability to be reused have been assessed, the optimal heterogeneous catalyst 1.10wt%Ni@BpyMP-1 was further evaluated with various substrates using 1 mol% of nickel compared to heteroarene (Scheme 4 and Scheme 5). Applying other iodoarenes in the arylation of benzothiophene (Scheme 4) shows that *p*-^{t}Bu substituent slightly increases the yield of the corresponding 2-arylbenzothiophene (54%). In turn, using *p*-iodoanisole leads to a drastic decrease in yield (11%). Although the yield is lower for these substrates when compared to the homogeneous reaction,[27] the selectivity between arylated benzothiophene and arylated-HMDS by product is significantly improved (see Table S3).

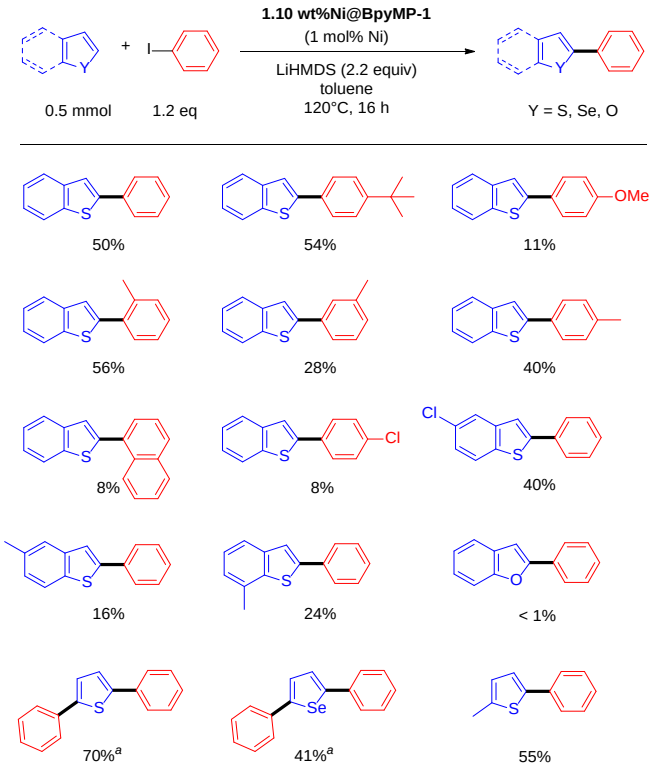

Scheme 4. Heterogeneous Ni-catalyzed direct C2 arylation of benzothiophenes, thiophene, selenophene and benzofuran. ([a] 2.4 equivalents of iodobenzene are used).

For thiophene and 2-methylthiophene, the corresponding arylation products could be isolated in average to good yields (Scheme 4). More scarcely studied selenophene, an attractive motif for optoelectronics[19] and bioactive compounds,[57] could also be successfully arylated (Scheme 4). When compared to the homogeneous reaction performed under otherwise identical conditions, the heterogenization of the catalyst gives rise to a significant increase in catalytic activity for both thiophene and selenophene as substrate (Scheme 4), with respectively 70% and 41% yield using 1.1wt%Ni@BpyMP-1 compared to 43% and 20% yield when using the homogeneous Ni(bpy)Cl_2.[27]
Benzofuran, which was reported as a possible coupling partner for this reaction under homogeneous conditions,[27] did not undergo arylation under these heterogeneous conditions, however without clear rationale (Scheme 4).
Finally, we found that molecular nickel complexes were also able to catalyze the direct arylation of indole in the presence of LiHMDS, although with a lower selectivity (Scheme 5). In the particular case of free (NH)-indole, the C3 selectivity might be explained in the light of a LiHMDS-mediated mechanism, as previously reported by our group for the Pd catalyzed reaction.[58] Using Ni(glyme)Cl_2 as catalyst, the yield in 3-phenyl-indole was low (11%) and the *N*-arylation was observed as a slightly preferred reaction (14% yield). Yield and selectivity could be slightly improved using bpy as a ligand (27% yield and 56% C3 selectivity over *N*-arylation).

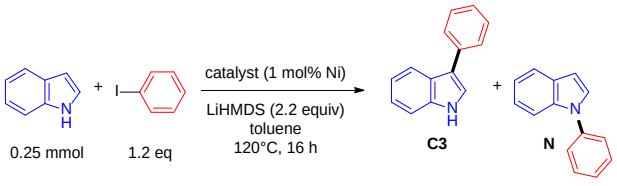

catalyst	C3 yield	N yield	C3 selectivity
Ni(glyme)Cl_2	11%	14%	44%
Ni(bpy)Cl_2	27%	21%	57%
Ni@BpyMP-1	**41%**	**25%**	**62%**

Scheme 5. Direct C3 *vs* *N*-arylation of indole by using homogeneous and heterogenized Ni molecular catalyst within BpyMP-1 porous macroligand.

Further improvement was made through heterogenization within BpyMP-1 as porous macroligand resulting in 41% yield in 3-phenyl-indole and 62% C3 selectivity over *N*-arylation when the Ni@BpyMP-1 catalyst was used under the same conditions. As observed for the arylation of benzothiophene, the incorporation of the catalyst within the porous polymer also significantly suppresses the formation of Ph-HMDS. This first example of heterogeneous Ni-catalyzed free (NH)-indole C3-H arylation opens promising perspective and is still under investigation to unravel the role of the porous macroligand for promoting regioselectivity.

3. CONCLUSIONS

We demonstrate here the heterogeneously catalyzed direct and fully regioselective C2-H arylation of various heteroarenes, including benzothiophene as an important building block for APIs. We also report the first proof-of-principle protocol for its efficient regeneration. The catalyst was designed by covalently integrating an earth-abundant nickel catalyst into the matrix of a porous organic polymer used as a porous macroligand. The coordination of the macroligand towards Ni was elucidated by combining IR and solid-state NMR spectroscopy with DFT calculations. The optimized heterogeneous catalytic system has been reused for at least seven times with a total TON of ca. 300 and a productivity of 12 grams of 2-phenylbenzothiophene per gram of catalyst without significant Ni leaching. The applicability of this novel heterogeneous system was further demonstrated by successfully arylating other heterocycles like thiophenes, selenophene and indole. Taking into account their robustness and their potential processability, the porous organic polymers used as macroligands for molecular catalysts further pave the way to molecularly defined and robust heterogeneous systems for a more sustainable synthesis of fine chemicals.

4. EXPERIMENTAL SECTION

Catalysts synthesis. For a typical Ni@BpyMP-1 synthesis, 100.0 mg (0.67 mmol) 1,3,5-triethynylbenzene, 310.3 mg (0.75 mmol) 4,4'-diiodobiphenyl, 80.0 mg (0.25 mmol) 5,5'-dibromo-2,2'-bipyridine and 15.5 mg (13.3 µmol) $Pd(PPh_3)_4$ were added to a flame dried glass reactor inside a glovebox.[29] The glass reactor was sealed with a Teflon septum. Outside the glovebox, 12 ml of anhydrous DMF and 6 ml of anhydrous NEt_3 were added and the reactor was placed in an oil bath. The reaction mixture was heated to 100°C for 24 h. The solid was purified by Soxhlet extraction using $CHCl_3$ for 6 h and using MeOH overnight. The yellow solid was dried at 80°C under vacuum (typically 220 mg). Then, 50 mg of polymer were dispersed in

2 ml of degassed methanol, then the desired amount of Ni(glyme)Cl_2 in 3 ml of dry methanol was added and the suspension was stirred for 3 d at 50°C. The supernatant was removed by centrifugation and the solid washed with anhydrous MeOH during 2 days (exchange with fresh MeOH every 12 h). The solid was dried under reduced pressure, first at room temperature and then at 80°C.

Catalysis. In a typical catalysis experiment, benzothiophene (34.4 mg, 0.25 mmol), LiHMDS (95 mg, 0.55 mmol, 2.2 equiv) and Ni@BpyMP-1 (13.5 mg) were added to a flame-dried Schlenk tube equipped with a magnetic stir bar inside a glove box. The flask was sealed with a silicon septum and transferred out of the glove box. Dry toluene (2 mL) was injected through the septum and the mixture was stirred for two minutes. Then iodobenzene (35 µl, 0.3 mmol, 1.2 equiv) and dodecane (40 µl, 0.174 mmol) as an internal standard for GC-FID analysis were injected through the septum. The reaction was stirred and heated to 120°C. After 16 h, the reaction mixture was quenched with 2 mL of dry methanol. The catalyst was separated by centrifugation and washed twice with dry methanol. The combined organic phases were evaporated and the crude product was purified by liquid size exclusion chromatography equipped with PLGel columns (10 µm, 50 Å) and using chloroform as eluent to obtain the isolated product.

AUTHOR INFORMATION

Corresponding Authors

* E-mail: jerome.canivet@ircelyon.univ-lyon1.fr ; florian.wisser@chemie.uni-regensburg.de

Author Contributions

The manuscript was written through contributions of all authors.

ACKNOWLEDGMENT

This work has been carried out within the H-CCAT project that has received funding from the European Union's Horizon 2020 research and innovation program under grant agreement No 720996. F.M.W. gratefully acknowledges financial support from the Deutsche Forschungsgemeinschaft (DFG, grant number WI 4721/3-1) and from CNRS through Momentum 2018 excellence grant. The authors are very grateful to IRCELYON scientific services and to Prof. Dr. G. Kickelbick (Saarland University) for providing access to CHN-analysis.

REFERENCES

(1) Gaich, T.; Baran, P. S. Aiming for the Ideal Synthesis. *J. Org. Chem.* **2010**, *75* (14), 4657–4673. https://doi.org/10.1021/jo1006812.

(2) Hendrickson, J. B. Systematic Synthesis Design. IV. Numerical Codification of Construction Reactions. *J. Am. Chem. Soc.* **1975**, *97* (20), 5784–5800. https://doi.org/10.1021/ja00853a023.

(3) Cano, R.; Schmidt, A. F.; McGlacken, G. P. Direct Arylation and Heterogeneous Catalysis; Ever the Twain Shall Meet. *Chem Sci* **2015**, *6* (10), 5338–5346. https://doi.org/10.1039/C5SC01534K.

(4) Santoro, S.; Kozhushkov, S. I.; Ackermann, L.; Vaccaro, L. Heterogeneous Catalytic Approaches in C–H Activation Reactions. *Green Chem* **2016**, *18* (12), 3471–3493. https://doi.org/10.1039/C6GC00385K.

(5) Pototschnig, G.; Maulide, N.; Schnürch, M. Direct Functionalization of C−H Bonds by Iron, Nickel, and Cobalt Catalysis. *Chem. - Eur. J.* **2017**, *23* (39), 9206–9232. https://doi.org/10.1002/chem.201605657.

(6) Gandeepan, P.; Müller, T.; Zell, D.; Cera, G.; Warratz, S.; Ackermann, L. 3d Transition Metals for C-H Activation. *Chem. Rev.* **2019**, *119* (4), 2192–2452. https://doi.org/10.1021/acs.chemrev.8b00507.

(7) Hayler, J. D.; Leahy, D. K.; Simmons, E. M. A Pharmaceutical Industry Perspective on Sustainable Metal Catalysis. *Organometallics* **2019**, *38* (1), 36–46. https://doi.org/10.1021/acs.organomet.8b00566.

(8) Bullock, R. M.; Chen, J. G.; Gagliardi, L.; Chirik, P. J.; Farha, O. K.; Hendon, C. H.; Jones, C. W.; Keith, J. A.; Klosin, J.; Minteer, S. D.; Morris, R. H.; Radosevich, A. T.; Rauchfuss, T. B.; Strotman, N. A.; Vojvodic, A.; Ward, T. R.; Yang, J. Y.; Surendranath, Y. Using Nature's Blueprint to Expand Catalysis with Earth-Abundant Metals. *Science* **2020**, *369* (6505). https://doi.org/10.1126/science.abc3183.

(9) Gandeepan, P.; Müller, T.; Zell, D.; Cera, G.; Warratz, S.; Ackermann, L. 3d Transition Metals for C–H Activation. *Chem. Rev.* **2019**, *119* (4), 2192–2452. https://doi.org/10.1021/acs.chemrev.8b00507.

(10) Stepek, I. A.; Itami, K. Recent Advances in C–H Activation for the Synthesis of π-Extended Materials. *ACS Mater. Lett.* **2020**. https://doi.org/10.1021/acsmaterialslett.0c00206.

(11) Gensch, T.; James, M. J.; Dalton, T.; Glorius, F. Increasing Catalyst Efficiency in C−H Activation Catalysis. *Angew. Chem. Int. Ed.* **2018**, *57* (9), 2296–2306. https://doi.org/10.1002/anie.201710377.

(12) Morgan, D.; Yarwood, S. J.; Barker, G. Recent Developments in C−H Functionalisation of Benzofurans and Benzothiophenes. *Eur. J. Org. Chem.* **2020**. https://doi.org/10.1002/ejoc.202001470.

(13) Dadiboyena, S. Recent Advances in the Synthesis of Raloxifene: A Selective Estrogen Receptor Modulator. *Eur. J. Med. Chem.* **2012**, *51*, 17–34. https://doi.org/10.1016/j.ejmech.2012.02.021.

(14) Keri, R. S.; Chand, K.; Budagumpi, S.; Balappa Somappa, S.; Patil, S. A.; Nagaraja, B. M. An Overview of Benzo[b]Thiophene-Based Medicinal Chemistry. *Eur. J. Med. Chem.* **2017**, *138*, 1002–1033. https://doi.org/10.1016/j.ejmech.2017.07.038.

(15) Delmas, P. D. Treatment of Postmenopausal Osteoporosis. *The Lancet* **2002**, *359* (9322), 2018–2026. https://doi.org/10.1016/S0140-6736(02)08827-X.

(16) Ebata, H.; Izawa, T.; Miyazaki, E.; Takimiya, K.; Ikeda, M.; Kuwabara, H.; Yui, T. Highly Soluble [1]Benzothieno[3,2-b]Benzothiophene (BTBT) Derivatives for High-Performance, Solution-Processed Organic Field-Effect Transistors. *J. Am. Chem. Soc.* **2007**, *129* (51), 15732–15733. https://doi.org/10.1021/ja074841i.

(17) Reddy, M. R.; Kim, H.; Kim, C.; Seo, S. 2-Thiopene[1]Benzothieno[3,2-b]Benzothiophene Derivatives as Solution-Processable Organic Semiconductors for Organic Thin-Film Transistors. *Synth. Met.* **2018**,

235, 153–159. https://doi.org/10.1016/j.synthmet.2017.12.012.

(18) Yao, H.; Ye, L.; Zhang, H.; Li, S.; Zhang, S.; Hou, J. Molecular Design of Benzodithiophene-Based Organic Photovoltaic Materials. *Chem. Rev.* **2016**, *116* (12), 7397–7457. https://doi.org/10.1021/acs.chemrev.6b00176.

(19) Wang, C.; Dong, H.; Hu, W.; Liu, Y.; Zhu, D. Semiconducting π-Conjugated Systems in Field-Effect Transistors: A Material Odyssey of Organic Electronics. *Chem. Rev.* **2012**, *112* (4), 2208–2267. https://doi.org/10.1021/cr100380z.

(20) Rej, S.; Das, A.; Chatani, N. Strategic Evolution in Transition Metal-Catalyzed Directed C–H Bond Activation and Future Directions. *Coord. Chem. Rev.* **2020**, 213683. https://doi.org/10.1016/j.ccr.2020.213683.

(21) Liégault, B.; Lapointe, D.; Caron, L.; Vlassova, A.; Fagnou, K. Establishment of Broadly Applicable Reaction Conditions for the Palladium-Catalyzed Direct Arylation of Heteroatom-Containing Aromatic Compounds. *J. Org. Chem.* **2009**, *74* (5), 1826–1834. https://doi.org/10.1021/jo8026565.

(22) Colletto, C.; Panigrahi, A.; Fernández-Casado, J.; Larrosa, I. Ag(I)–C–H Activation Enables Near-Room-Temperature Direct α-Arylation of Benzo[b]Thiophenes. *J. Am. Chem. Soc.* **2018**, *140* (30), 9638–9643. https://doi.org/10.1021/jacs.8b05361.

(23) El Kazzouli, S.; Koubachi, J.; El Brahmi, N.; Guillaumet, G. Advances in Direct C–H Arylation of 5,5- 6,5- and 6,6-Fused-Heterocycles Containing Heteroatoms (N, O, S). *RSC Adv.* **2015**, *5* (20), 15292–15327. https://doi.org/10.1039/C4RA15384G.

(24) Mao, S.; Li, H.; Shi, X.; Soulé, J.; Doucet, H. Environmentally Benign Arylations of 5-Membered Ring Heteroarenes by Pd-Catalyzed C−H Bonds Activations. *ChemCatChem* **2019**, *11* (1), 269–286. https://doi.org/10.1002/cctc.201801448.

(25) Do, H.-Q.; Khan, R. M. K.; Daugulis, O. A General Method for Copper-Catalyzed Arylation of Arene C−H Bonds. *J. Am. Chem. Soc.* **2008**, *130* (45), 15185–15192. https://doi.org/10.1021/ja805688p.

(26) Doba, T.; Matsubara, T.; Ilies, L.; Shang, R.; Nakamura, E. Homocoupling-Free Iron-Catalysed Twofold C–H Activation/Cross-Couplings of Aromatics via Transient Connection of Reactants. *Nat. Catal.* **2019**, *2* (5), 400–406. https://doi.org/10.1038/s41929-019-0245-3.

(27) Mohr, Y.; Hisler, G.; Grousset, L.; Roux, Y.; Alessandra Quadrelli, E.; M. Wisser, F.; Canivet, J. Nickel-Catalyzed and Li-Mediated Regiospecific C–H Arylation of Benzothiophenes. *Green Chem.* **2020**, *22* (10), 3155–3161. https://doi.org/10.1039/D0GC00917B.

(28) Wisser, F. M.; Mohr, Y.; Quadrelli, E. A.; Canivet, J. Porous Macroligands: Materials for Heterogeneous Molecular Catalysis. *ChemCatChem* **2020**, *12* (5), 1270–1275. https://doi.org/10.1002/cctc.201902064.

(29) Wisser, F. M.; Berruyer, P.; Cardenas, L.; Mohr, Y.; Quadrelli, E. A.; Lesage, A.; Farrusseng, D.; Canivet, J. Hammett Parameter in Microporous Solids as Macroligands for Heterogenized Photocatalysts. *ACS Catal.* **2018**, *8* (3), 1653–1661. https://doi.org/10.1021/acscatal.7b03998.

(30) Wisser, F. M.; Duguet, M.; Perrinet, Q.; Ghosh, A. C.; Alves-Favaro, M.; Mohr, Y.; Lorentz, C.; Quadrelli, E. A.; Palkovits, R.; Farrusseng, D.; Mellot-Draznieks, C.; Waele, V. de; Canivet, J. Molecular Porous Photosystems Tailored for Long-Term Photocatalytic CO2 Reduction. *Angew. Chem. Int. Ed.* **2020**, *59*, 5116–5122. https://doi.org/10.1002/anie.201912883.

(31) Quan, Y.; Song, Y.; Shi, W.; Xu, Z.; Chen, J. S.; Jiang, X.; Wang, C.; Lin, W. Metal–Organic Framework with Dual Active Sites in Engineered Mesopores for Bioinspired Synergistic Catalysis. *J. Am. Chem. Soc.* **2020**, *142* (19), 8602–8607. https://doi.org/10.1021/jacs.0c02966.

(32) Canivet, J.; Bernoud, E.; Bonnefoy, J.; Legrand, A.; Todorova, T.; Quadrelli, E. A.; Mellot-Draznieks, C. Synthetic and Computational Assessment of a Chiral Metal-Organic Framework Catalyst for Predictive Asymmetric Transformation. *Chem. Sci.* **2020**, *11*, 8800–8808. https://doi.org/10.1039/D0SC03364B.

(33) Zhou, T.-Y.; Auer, B.; Lee, S. J.; Telfer, S. G. Catalysts Confined in Programmed Framework Pores Enable New Transformations and Tune Reaction Efficiency and Selectivity. *J. Am. Chem. Soc.* **2019**, *141* (4), 1577–1582. https://doi.org/10.1021/jacs.8b11221.

(34) Kim, M. J.; Ahn, S.; Yi, J.; Hupp, J. T.; Notestein, J. M.; Farha, O. K.; Lee, S. J. Ni(II) Complex on a Bispyridine-Based Porous Organic Polymer as a Heterogeneous Catalyst for Ethylene Oligomerization. *Catal. Sci. Technol.* **2017**, *7* (19), 4351–4354. https://doi.org/10.1039/c7cy01274h.

(35) Dong, Y.; Jv, J.-J.; Li, Y.; Li, W.-H.; Chen, Y.-Q.; Sun, Q.; Ma, J.-P.; Dong, Y.-B. Nickel-Metalated Porous Organic Polymer for Suzuki–Miyaura Cross-Coupling Reaction. *RSC Adv.* **2019**, *9* (35), 20266–20272. https://doi.org/10.1039/C9RA03679B.

(36) Ohno, A.; Sato, T.; Mase, T.; Uozumi, Y.; Yamada, Y. M. A. A Convoluted Polyvinylpyridine-Palladium Catalyst for Suzuki-Miyaura Coupling and C−H Arylation. *Adv. Synth. Catal.* **2020**, *362* (21), 4687–4698. https://doi.org/10.1002/adsc.202000742.

(37) Iwai, T.; Harada, T.; Shimada, H.; Asano, K.; Sawamura, M. A Polystyrene-Cross-Linking Bisphosphine: Controlled Metal Monochelation and Ligand-Enabled First-Row Transition Metal Catalysis. *ACS Catal.* **2017**, *7* (3), 1681–1692. https://doi.org/10.1021/acscatal.6b02988.

(38) Wisser, F. M.; Mohr, Y.; Quadrelli, E. A.; Farrusseng, D.; Canivet, J. Microporous Polymers as Macroligands for Pentamethylcyclopentadienylrhodium Transfer-Hydrogenation Catalysts. *ChemCatChem* **2018**, *10* (8), 1778–1782. https://doi.org/10.1002/cctc.201701836.

(39) Trunk, M.; Herrmann, A.; Bildirir, H.; Yassin, A.; Schmidt, J.; Thomas, A. Copper-Free Sonogashira Coupling for High-Surface-Area Conjugated Microporous Poly(Aryleneethynylene) Networks. *Chem. - Eur. J.* **2016**, *22* (21), 7179–7183. https://doi.org/10.1002/chem.201600783.

(40) Patzke, B.; Stanger, A. Synthesis, Characterization, and Reactions of the New Seven-Membered Nickelacycle (2,2‘-Bipyridine)-6,7-Dihydro-5 H -Dibenzo[c,e]Nickelepine. *Organometallics* **1996**, *15* (11), 2633–2639. https://doi.org/10.1021/om9509812.

(41) Schlüter, A. D.; Bo, Z. Synthesis of Conjugated Polymers for Materials Science. In *Handbook of Organopalladium Chemistry for Organic Synthesis*; Negishi, E., Ed.; Wiley & Sons, Inc., 2002; pp 825–861.

(42) Johnson, R. L.; Schmidt-Rohr, K. Quantitative Solid-State 13C NMR with Signal Enhancement by Multiple Cross Polarization. *J. Magn. Reson.* **2014**, *239*, 44–49. https://doi.org/10.1016/j.jmr.2013.11.009.

(43) Duan, P.; Schmidt-Rohr, K. Composite-Pulse and Partially Dipolar Dephased MultiCP for Improved Quantitative Solid-State 13C NMR. *J. Magn. Reson.* **2017**, *285*, 68–78. https://doi.org/10.1016/j.jmr.2017.10.010.

(44) Pell, A. J.; Pintacuda, G.; Grey, C. P. Paramagnetic NMR in Solution and the Solid State. *Prog. Nucl. Magn. Reson. Spectrosc.* **2019**, *111*, 1–271. https://doi.org/10.1016/j.pnmrs.2018.05.001.

(45) Klein, N.; Hoffmann, H. C.; Cadiau, A.; Getzschmann, J.; Lohe, M. R.; Paasch, S.; Heydenreich, T.; Adil, K.; Senkovska, I.; Brunner, E.; Kaskel, S. Structural Flexibility and Intrinsic Dynamics in the M2(2,6-Ndc)2(Dabco) (M = Ni, Cu, Co, Zn) Metal–Organic Frameworks. *J. Mater. Chem.* **2012**, *22* (20), 10303–10312. https://doi.org/10.1039/C2JM15601F.

(46) Xiang, Y.; Dong, W.; Wang, P.; Wang, S.; Ding, X.; Ichihara, F.; Wang, Z.; Wada, Y.; Jin, S.; Weng, Y.; Chen, H.; Ye, J. Constructing Electron Delocalization Channels in Covalent Organic Frameworks Powering CO2 Photoreduction in Water. *Appl. Catal. B Environ.* **2020**, *274*, 119096. https://doi.org/10.1016/j.apcatb.2020.119096.

(47) Massiot, D.; Fayon, F.; Capron, M.; King, I.; Calvé, S. L.; Alonso, B.; Durand, J.-O.; Bujoli, B.; Gan, Z.; Hoatson, G. Modelling One- and Two-Dimensional Solid-State NMR Spectra. *Magn. Reson. Chem.* **2002**, *40* (1), 70–76. https://doi.org/10.1002/mrc.984.

(48) Castellucci, E.; Angeloni, L.; Neto, N.; Sbrana, G. IR and Raman Spectra of A 2,2′-Bipyridine Single Crystal: Internal Modes. *Chem. Phys.* **1979**, *43* (3), 365–373. https://doi.org/10.1016/0301-0104(79)85204-0.

(49) Gerasimova, T. P.; Katsyuba, S. A. Bipyridine and Phenanthroline IR-Spectral Bands as Indicators of Metal Spin State in Hexacoordinated Complexes of Fe(II), Ni(II) and Co(II). *Dalton Trans.* **2013**, *42* (5), 1787–1797. https://doi.org/10.1039/C2DT31922E.

(50) Niven, M. L.; Percy, G. C. The Infrared Spectra (3500-140 Cm−1) of the 2,2'-Bipyridine, 2-Aminomethylpyridine and Ethylenediamine Adducts and the Sodium Tris-Compounds of Cobalt(II), Nickel(II) and Zinc(II) Acetylacetonates. *Transit. Met. Chem.* **1978**, *3* (1), 267–271. https://doi.org/10.1007/BF01393566.

(51) Crabtree, R. H. Deactivation in Homogeneous Transition Metal Catalysis: Causes, Avoidance, and Cure. *Chem. Rev.* **2015**, *115* (1), 127–150. https://doi.org/10.1021/cr5004375.

(52) Kharitonov, D. N.; Golubeva, E. N. Role of Catalyst Deactivation and Regeneration in the Heck Reaction Involving Unactivated Aryl Bromides. *Kinet. Catal.* **2005**, *46* (1), 47–51. https://doi.org/10.1007/PL00021984.

(53) Faust, M.; Bryan, A. M.; Mansikkamäki, A.; Vasko, P.; Olmstead, M. M.; Tuononen, H. M.; Grandjean, F.; Long, G. J.; Power, P. P. The Instability of NiN(SiMe3)22: A Fifty Year Old Transition Metal Silylamide Mystery. *Angew. Chem. Int. Ed.* **2015**, *54* (44), 12914–12917. https://doi.org/10.1002/anie.201505518.

(54) Standley, E. A.; Jamison, T. F. Simplifying Nickel(0) Catalysis: An Air-Stable Nickel Precatalyst for the Internally Selective Benzylation of Terminal Alkenes. *J. Am. Chem. Soc.* **2013**, *135* (4), 1585–1592. https://doi.org/10.1021/ja3116718.

(55) Kim, Y.; Iwai, T.; Fujii, S.; Ueno, K.; Sawamura, M. Dumbbell-Shaped 2,2'-Bipyridines: Controlled Metal Monochelation and Application to Ni-Catalyzed Cross-Couplings. *Chem. – Eur. J.* **2020**. https://doi.org/10.1002/chem.202004053.

(56) Harry, N. A.; Saranya, S.; Ujwaldev, S. M.; Anilkumar, G. Recent Advances and Prospects in Nickel-Catalyzed C–H Activation. *Catal. Sci. Technol.* **2019**, *9* (8), 1726–1743. https://doi.org/10.1039/C9CY00009G.

(57) Mahmoud, A. B. A.; Kirsch, G.; Peagle, E. Biologically Active Selenophenes and Benzo[b]Selenophenes. *Curr. Org. Synth.* **2017**, *14* (8), 1091–1101. https://doi.org/10.2174/1570179414666170601121832.

(58) Mohr, Y.; Renom-Carrasco, M.; Demarcy, C.; Quadrelli, E. A.; Camp, C.; Wisser, F. M.; Clot, E.; Thieuleux, C.; Canivet, J. Regiospecificity in Ligand-Free Pd-Catalyzed C–H Arylation of Indoles: LiHMDS as Base and Transient Directing Group. *ACS Catal.* **2020**, *10* (4), 2713–2719. https://doi.org/10.1021/acscatal.9b04864.

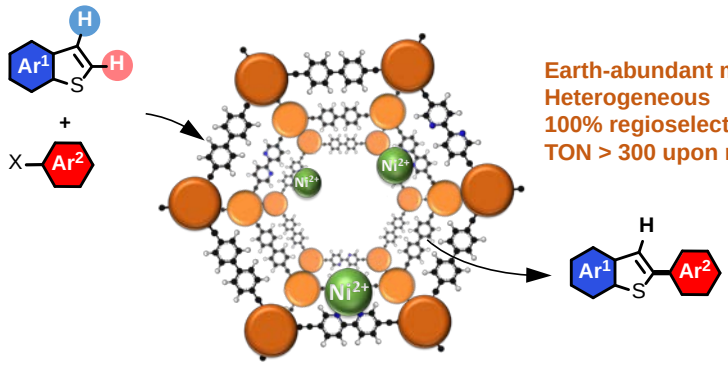

Earth-abundant metal
Heterogeneous
100% regioselective
TON > 300 upon recycling